EPJ Web of Conferences **66**, 06007 (2014)
DOI: 10.1051/epjconf/ 20146606007

Nonperturbative charm content of the nucleon

T. J. Hobbs[1,a], J. T. Londergan[1], and W. Melnitchouk[2]

[1] *Department of Physics and Center for the Exploration of Energy and Matter, Indiana University, Bloomington, IN 47405, USA*
[2] *Jefferson Lab, Newport News, VA 23606, USA*

Abstract. We propose a new meson-baryon model for intrinsic charm in the proton. Particular attention is paid to the existence and persistence of high x behavior, especially in the structure function $F_2^{c\bar{c}}(x, Q^2)$.

An understanding of nonperturbative effects at large x is crucially important to a variety of efforts to explore QCD and its implications. Whether for precision flavor physics at the LHC or proposed facilities, searches for potential dark matter candidates, or efforts to constrain DIS parton distributions more robustly, a clearer picture of heavy quark production and evolution is essential, particularly regarding the behavior of charm in the proton.

The prevailing picture at present (and as deployed in typical analyses) is one in which threshold charm ($Q^2 \sim m_c^2$) arises at LO through the pQCD mechanism of boson-gluon fusion, and evolves at higher Q^2 in a standard DGLAP gluon-splitting process. In both cases, the resulting charm PDF closely depends upon the gluon density, and is therefore sharply peaked at low x.

In contrast to these perturbative mechanisms, nonperturbative or *intrinsic* charm (IC) might play a rôle through the action of soft gluon exchanges or Fock-space expansions of the proton into five-quark states involving $c, \bar{c}$ [1]. Additionally, the proton might undergo hadronic fluctuations into (anti-)charm-containing configurations of mesons and baryons, admitting some non-zero $c(x, m_c^2) \neq \bar{c}(x, m_c^2)$ before QCD evolution can generate an *extrinsic* charm component. Such representations might be referred to broadly as meson-baryon models (MBMs) of the interacting nucleon.

While there have been previous attempts [2] to compute IC distributions using MBMs, these have not consistently included physical degrees of freedom in the form of spin and isospin, and have ignored contributions from higher-mass hadronic states, which we find to have a significant effect. Here we describe the major results of a new calculation that repairs these defects [3].

Nonperturbative charm may enter the proton due to spontaneous, short-lived fluctuations of the nucleon into states with a virtual meson M and baryon B,

$$|N\rangle \;=\; \sqrt{Z}\,|N\rangle_0 \;+\; \sum_{M,B} \int dy\, d^2\boldsymbol{k}_\perp\, \phi_{MB}(y, \boldsymbol{k}_\perp^2)\, |M(y, \boldsymbol{k}_\perp); B(\bar{y}, -\boldsymbol{k}_\perp)\rangle, \tag{1}$$

in which $|N\rangle_0$ is the "bare" state of three light quarks, and Z is a wave function renormalization. We use time-ordered perturbation theory (TOPT) to calculate the functions $\phi_{MB}(y, \boldsymbol{k}_\perp^2)$, which give probability amplitudes for the interacting nucleon to be in states containing a virtual meson M with

[a] e-mail: timjhobb@indiana.edu

longitudinal momentum fraction y and transverse momentum $\boldsymbol{k}_\perp$, and a baryon B with longitudinal momentum fraction $\bar{y} = 1 - y$ and transverse momentum $-\boldsymbol{k}_\perp$. The total invariant mass squared of the meson–baryon system s_{MB} can be written in the infinite momentum frame (IMF) as

$$s_{MB}(y, \boldsymbol{k}_\perp^2) = \frac{m_M^2 + \boldsymbol{k}_\perp^2}{y} + \frac{M_B^2 + \boldsymbol{k}_\perp^2}{1 - y}, \tag{2}$$

where m_M and M_B are the meson and baryon masses, respectively. To determine an overall level of

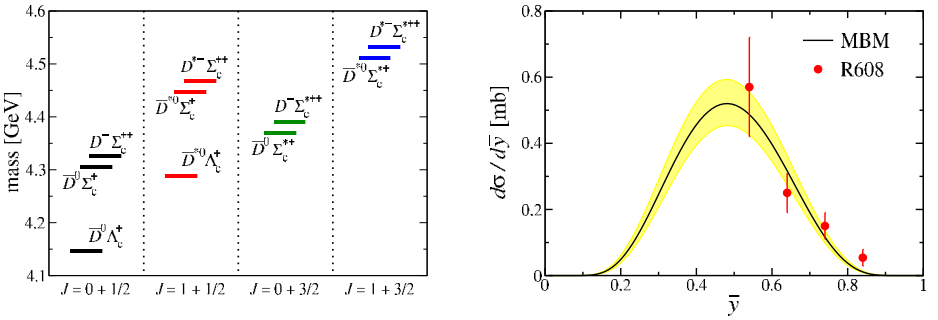

Figure 1. (Left) Hadronic states contributing to the incoherent sum of Eq. 3. (Right) MBM fit of R608 data.

IC, we consider those meson–baryon states that contain $c, \bar{c}$ as illustrated in the left of Figure 1; the resulting probability distributions for anticharm (and charm) are convolutions of the form,

$$\bar{c}(x) \;=\; \sum_{M,B} \Big[\int_x^1 \frac{dy}{y}\, f_{MB}(y)\, \bar{c}_M(x/y) + \int_x^1 \frac{d\bar{y}}{\bar{y}}\, f_{BM}(\bar{y})\, \bar{c}_B(x/\bar{y}) \Big], \tag{3}$$

where for ease of notation we have omitted the dependence of the distributions on the scale Q^2. Analogous relations hold for the charm distributions.

The contributions of individual hadronic configurations to the IC distributions of Eq. 3 are controlled by the splitting functions $f_{MB}(y)$, which are trivially related to the $\phi_{MB}(y, \boldsymbol{k}_\perp^2)$ amplitudes of Eq. 1 by $\boldsymbol{k}_\perp^2$-integration. Moreover, momentum conservation forces these probability distributions to obey the symmetry relation $f_{MB}(y) = f_{BM}(\bar{y})$.

As an illustration, we find that the dominant term in the sum of Eq. 3 comes from the vector dissociation $p \to \bar{D}^{*0}\Lambda_c^+$:

$$\begin{aligned} f_{D^*\Lambda_c}(y) \;=\; & \frac{1}{16\pi^2} \int \frac{d\boldsymbol{k}_\perp^2}{y(1-y)} \frac{|F(s_{D^*\Lambda_c})|^2}{(s_{D^*\Lambda_c} - M^2)^2} \\ & \times \Big[g^2\, G_v(y, \boldsymbol{k}_\perp^2) \;+\; g\frac{f}{M}\, G_{vt}(y, \boldsymbol{k}_\perp^2) \;+\; \frac{f^2}{M^2}\, G_t(y, \boldsymbol{k}_\perp^2) \Big], \end{aligned} \tag{4}$$

in which M represents the proton mass, the hadronic coupling constants g, f assume an SU(4) quark model symmetry as in previous analyses of DN scattering amplitudes [4], and divergences are regulated by a form factor $F(s_{MB}) = \exp\left(-(s_{MB} - M^2)/\Lambda^2\right)$. The trace terms G_v, G_{vt}, and G_t are obtained by calculating the proper numerator algebra in TOPT diagrams that result from the vector-tensor interaction we assume in the relevant meson-baryon Lagrangian. Applying the same TOPT methodology

to all permitted charm-state dissociations of the proton allows a model prediction for production of Λ_c in pp collisions using

$$E\frac{d\sigma^{pp\to\Lambda_c X}}{d\bar{y}} = \frac{\bar{y}}{\pi}\sum_M f_{\Lambda_c M}(\bar{y})\,\sigma^{Mp}_{total}(sy); \tag{5}$$

with this, we can tune the universal cutoff parameter Λ that enters Eq. 4 through the form factor $F(s_{MB})$ until achieving maximum agreement with the R608 data [5] shown in the righthand panel of Figure 1. We find $\Lambda = (3.0 \pm 0.2)$ GeV, with the yellow band of Figure 1 corresponding to the purely statistical error about the central value.

We also require density functions for the charm content of the intermediate meson-baryon states to evaluate the convolutions of Eq. 3. Like the hadronic splitting functions $f_{MB}(y)$, these may be computed in TOPT after assuming a suitable Lagrangian of the form $\mathcal{L} = g\,\bar{\psi}_{\bar{c}}\gamma_\mu\psi_u\theta^\mu_{D^*}$ + h. c., such that the $\bar{c}$ distribution inside the vector $\bar{D}^*$ meson has the form

$$\begin{aligned}\bar{c}_{D^*}(z) &= \frac{N_{D^*}}{16\pi^2}\int\frac{d\hat{\boldsymbol{k}}^2_\perp}{[z(1-z)]^2}\frac{[F(s_{\bar{c}u})]^2}{(m^2_{D^*}-s_{\bar{c}u})^2}\Bigg(\Big(\frac{\hat{\boldsymbol{k}}^2_\perp+m^2_u}{m^2_{D^*}}+(1-z)^2\Big)(\hat{\boldsymbol{k}}^2_\perp+m^2_{\bar{c}}+z^2m^2_{D^*}) \\ &+ \hat{\boldsymbol{k}}^2_\perp+(zm_u+(1-z)m_{\bar{c}})^2+4z(1-z)m_um_{\bar{c}}\Bigg).\end{aligned} \tag{6}$$

This construction becomes numerically unstable as a result of the small size of the constituent mass of the charm quark relative to the physical $\bar{D}^*$ pole mass. We remedy this behavior by selecting a "confining" form factor

$$F(s_{\bar{c}u}) = (m^2_{D^*}-s_{\bar{c}u})\cdot\exp\left(\frac{m^2_{D^*}-s_{\bar{c}u}}{\Lambda^2}\right), \tag{7}$$

which cancels the energy denominator ordinarily present in the TOPT formalism, essentially prohibiting the decay of the vector meson into its internal quark degrees of freedom [6].

If we calculate the collection of splitting functions $f_{MB}(y)$ at the fitted value of the main model parameter $\Lambda = 3$ GeV as in the lefthand panel of Figure 2, it becomes apparent that the charm MBM is strongly dominated by a single state – the $\bar{D}^*\Lambda_c$, shown as a solid, red line. Note that the other curves in the left panel of Figure 2 have been rescaled relative to the $\bar{D}^*\Lambda_c$ line by powers of 10. The dominance of the $\bar{D}^*$ exchange may be understood as resulting from the interplay of the quark model coupling constants with a steep dependence on the Λ cutoff due to spin-1 tensor interactions contained in Eq. 4. The contribution of $\bar{D}^*\Lambda_c$ to the $\bar{c}$ distribution in the proton follows the convolution of Eqs. 4 and 6. In each case, (anti-)charm distributions inside meson-baryon states are normalized to preserve a zero first moment of the charm valence distribution $c(x)-\bar{c}(x)$. As such, the size of individual states' contribution to the MBM can be deduced from the magnitudes of the $f_{MB}(y)$ in Figure 2 — implying $\sim 70\%$ of the model derives from $\bar{D}^*\Lambda_c$.

We compute the electromagnetic structure function $F_2^{c\bar{c}}$ as

$$F_2^{c\bar{c}}(x,Q^2) = \frac{4x}{9}\Big[c(x,Q^2)+\bar{c}(x,Q^2)\Big], \tag{8}$$

finding it too is dominated by $\bar{D}^*$ exchange; in particular, Eq. 8 is evaluated using the full MBM with the confining form factor of Eq. 7 and $m_c = 1.3$ GeV, as shown in the right panel of Figure 2. The solid midline marks the model output at the central value of the fitted cutoff parameter, and the shaded band represents the complete uncertainty from the Λ_c production fits of Figure 1 — i.e., $\Lambda = (3.0 \pm 0.2)$ GeV. This family of curves comes from the evolution of the flavor singlet $c(x)+\bar{c}(x)$ distribution to $Q^2 = 60$ GeV^2 to make the given data comparison. Here, the $F_2^{c\bar{c}}$ calculation overhangs the purely

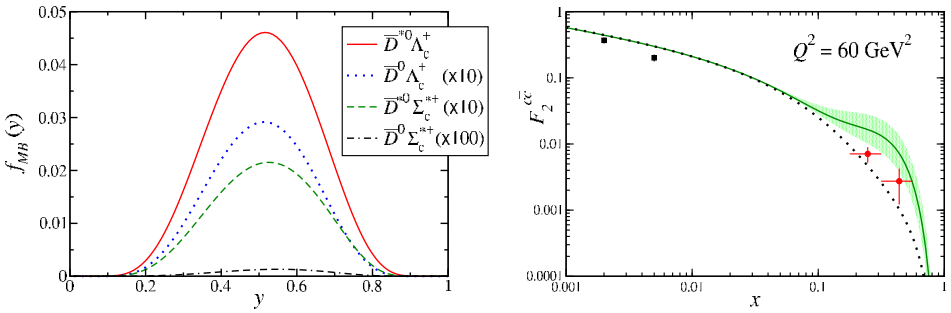

Figure 2. (Left) The hadronic splitting functions $f_{MB}(y)$ entering the MBM. (Right) $F_2^{c\bar{c}}$ as computed in the full MBM, and evolved via massless DGLAP to the scale of H1 and EMC measurements.

extrinsic result (dotted line) that follows from the massless evolution of an initial distribution with the boundary condition $c(x, m_c^2) = \bar{c}(x, m_c^2) = 0$; the large x "excess" becomes pronounced for $x \geq 0.1$, in a characteristic signal for nonperturbative charm. At low x, we compare with H1 data [7] as a check of the adequacy of the massless evolution, whereas the data in the high x valence region are from EMC [8]. The region of overlap between EMC uncertainties and the lower bounds of the computed error band suggests that intermediate Q^2 measurements may tolerate some IC at the level of $2.8 \leq \Lambda \leq 3.0$ GeV, as determined in our MBM. The overall size of IC represented by this range is best quantified by the numerical value of the moments $P_c^{(n)} = \int_0^1 dx x^n [c(x) + \bar{c}(x)]$. According to this definition, the total momentum carried by IC is $0.6\% \leq P_c^{(1)} \leq 1.4\%$ — rather small compared with the results of previous global analyses [9]. EMC at smaller Q^2 may impose still more stringent constraints to the level of IC awaiting a new global analysis [10] incorporating the framework here described.

TJH and JTL were supported in part by the US National Science Foundation under grants NSF-PHY-1205019 and NSF-PHY-0854805. The work of TJH was also supported in part by DOE grant DE-FG02-87ER40365. WM was supported by the DOE contract No. DE-AC05-06OR23177, under which Jefferson Science Associates, LLC operates Jefferson Lab.

References

[1] S. J. Brodsky, P. Hoyer, C. Peterson and N. Sakai, Phys. Lett. B **93**, 451 (1980).
[2] J. Pumplin, Phys. Rev. D **73**, 114015 (2006).
[3] T. J. Hobbs, J. T. Londergan and W. Melnitchouk, arXiv:1311.1578 [hep-ph].
[4] J. Haidenbauer, G. Krein, U.-G. Meißner and A. Sibirtsev, Eur. Phys. J. A **37**, 55 (2008).
[5] P. Chauvat *et al.* [R608 Collaboration], Phys. Lett. B **199**, 304 (1987).
[6] W. Melnitchouk, A. W. Schreiber and A. W. Thomas, Phys. Rev. D **49**, 1183 (1994).
[7] A. Aktas *et al.* [H1 Collaboration], Eur. Phys. J. C **45**, 23 (2006).
[8] J. J. Aubert *et al.* [European Muon Collaboration], Nucl. Phys. **B213**, 31 (1983); Phys. Lett. B **94**, 96 (1980); *ibid.* B **110**, 73 (1982).
[9] J. Pumplin, H. L. Lai and W. K. Tung, Phys. Rev. D **75**, 054029 (2007).
[10] T. J. Hobbs, P. Jimenez-Delgado, J. T. Londergan and W. Melnitchouk, in preparation (2014).